Geotechnical Aspects of Underground Construction in Soft Ground, Mair & Taylor (eds)
 ISBN 90 5410 856 8

Earth pressures acting on flexible circular shafts in sand

K.Ueno & Y.Yokoyama
Utsunomiya University, Japan
A.Ohi
Japan Highway Public Co., Hokkaido, Japan
T.Fujii
Nishimatsu Construction Co., Ltd, Tokyo, Japan

ABSTRACT: The authors investigated the effects of stiffness on the earth pressure acting on cylindrical vertical shafts in order to establish a shaft design method. For this purpose, the authors defined a quantity representing the stiffness of circular shafts and developed a new in-flight excavation technique for centrifuge model tests. The earth pressures acting on shafts of differing shaft stiffness and radii were measured under 100g of acceleration. According to the test results, Berezantzev's active earth pressure gives an underestimation, while Rankine's value is unduly conservative at deep sections. Furthermore, the stiffness of the shafts dominated the magnitude of the earth pressure acting on the shaft. A simple prediction method regarding the effects of shaft stiffness is proposed. The authors recommend that the effects of stiffness should be considered in the design method.

1 INTRODUCTION

The effects of stiffness of circular shafts on the earth pressure acting on the shafts themselves should be considered in the method of shaft design. Compared with gravity retaining walls, circular shafts installed in a level homogeneous ground may experience smaller horizontal displacements because of their symmetry. Therefore, it may be expected that the stress condition of the surrounding soil does not reach the active plastic state, and values of earth pressures become greater than active pressures. Furthermore as is well known among soil engineers, the stiffness of sheet piles strongly affects the earth pressure acting upon them.

Due to difficulties regarding the interaction between circular shafts and surrounding soils, the effects of shaft stiffness have not yet been clearly investigated. Although Coulomb and Rankine theories are used for current design codes for shafts in Japan because of their simplicity, these theories consider only two-dimensional problems. On the other hand, Terzaghi (1942) and Berezantzev (1958) suggested theoretical methods for circular vertical shafts. These theoretical methods treat only rigid perfectly plastic materials so that the effect of a static soil-structure interaction, including the effect of stiffness of shafts, is not considered. A proposed analysis of Wong and Kaiser (1988a) and an experimental examination by Fujii et al. (1994) considered a relationship between radial earth pressure and the displacement of shafts. No effect of the stiffness was, however, taken into account in these investigations.

To establish a prediction method taking account of the effects of stiffness of circular shafts on earth pressure, the authors defined a quantity representing the stiffness of circular shafts and developed a new in-flight excavation technique. The effects of stiffness of the shafts are discussed and a simple prediction method is proposed in this paper.

2 MODEL SHAFTS

Seven types of model cylindrical vertical shafts made of copper and/or acrylic were used in this study. Figure 1 shows notations to describe dimensions of a model shaft, where H is the height of the shaft; z, the depth; z_0, the embedded depth of the shaft; D, the excavation depth; t, the thickness of the shaft; R, the inner radius of the shaft. Subscripts m and p represent model and prototype dimensions respectively. The aspect ratio $z_0/2R$ expresses the ratio of a longitudinal length to a lateral length of the shaft. Shaft names, the materials and other parameters of shafts are tabulated in Table 1.

Apparent Young's modulus Et/R is defined hereby to represent the stiffness of shafts. The values are also listed in Table 1. According to an elastic thin tube theory (Roark and Young 1975), the increment of circumferential stress $\Delta\sigma_\theta$, acting in the thin tube subjected to an increment of differential radial pressure $\Delta(\sigma_{ro} - \sigma_{ri})$ and having a thickness smaller than a tenth of its radius, is

$$\Delta\sigma_\theta = \Delta(\sigma_{ro} - \sigma_{ri})\frac{R}{t} \qquad (1)$$

where σ_{ro} is the radial pressure acting on the outer surface of the shaft; σ_{ri}, the radial pressure acting on the inner surface of the shaft. Assuming linear elasticity and neglecting increments of other stress components, we obtain the relationship between stress increment $\Delta\sigma_\theta$ and strain increment $\Delta\varepsilon_\theta$,

$$\Delta\sigma_\theta = E\Delta\varepsilon_\theta \tag{2}$$

where E is Young's modulus. Deformation compatibility requires,

$$\Delta\varepsilon_\theta = \Delta\varepsilon_r \tag{3}$$

where $\Delta\varepsilon_r = \Delta R/R$. Substituting Eq. 2 and Eq. 3 into Eq. 1, we obtain an expression for the relationship between the increment of differential radial pressure $\Delta(\sigma_{ro} - \sigma_{ri})$ and the circumferential strain increment $\Delta\varepsilon_\theta$

$$\Delta(\sigma_{ro} - \sigma_{ri}) = \left(\frac{Et}{R}\right)\Delta\varepsilon_\theta \tag{4}$$

where (Et/R) is apparent Young's modulus.

The model shafts used were equipped with ten strain gauges which provided measurements of the circumferential strain increments $\Delta\varepsilon_\theta$ at five different depths, as shown with the small rectangles in Fig. 1. Applying the measurements of circumferential strain increments $\Delta\varepsilon_\theta$ into Eq. 4, we can obtain the increments of differential radial pressure $\Delta(\sigma_{ro} - \sigma_{ri})$ that would be induced during an in-flight excavation sequence.

Apparent Young's moduli of all model shafts prepared for this study were examined by using a triaxial cell prior to centrifuge model tests. The measured values of apparent Young's modulus agreed well with the theoretical values computed with Young's modulus of $E = 129$GPa. Figure 2 shows a comparison of the aspect ratio $z_0/2R$ and apparent Young's modulus Et/R between model shafts and actual shafts made of cast-in-place reinforced concrete in Japan. The model shafts that were prepared cover the range of higher aspect ratios $z_0/2R$ and lower apparent Young's moduli Et/R of actual cast-in-place reinforced concrete shafts.

Table 1: Model shafts

Name	Mat.	R_m (mm)	t_m (mm)	z_{0m} (mm)	Et/R (GPa)
OE1822	Copper	11.0	0.18	16.5	2.12
OE3036	Copper	18.0	0.30	16.5	2.16
OE2550	Copper	23.9	0.25	16.5	1.40
OE3050	Copper	23.9	0.30	16.5	1.72
OE4050	Copper	23.9	0.40	16.5	2.38
OE5050	Copper	23.9	0.50	16.5	2.58
OE30AC	Acrylic	23.9	3.00	16.5	0.392

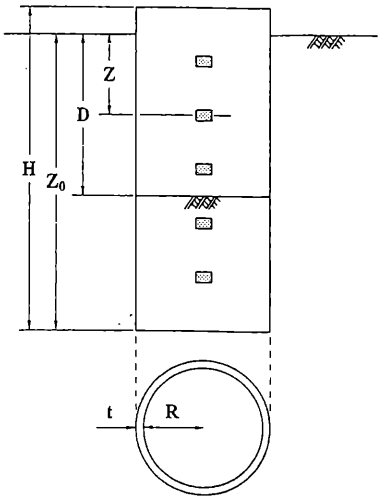

Fig. 1: Model shaft

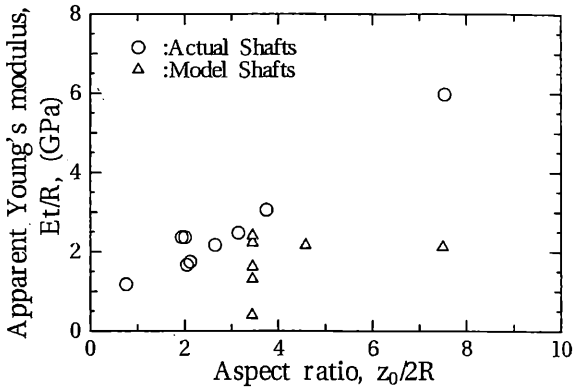

Fig. 2: Comparison between model shafts and actual shafts

3 APPARATUS AND PROCEDURE

The centrifuge used was a balanced beam centrifuge, having an effective radius of 1.18m, driven by a 11kW AC motor, located at Utsunomiya University. The test setup used consisted of a rectangular strong box made of steel plates and a special vacuum excavator. The rectangular strong box, with dimensions 500mm wide, 300mm deep and 200mm thick, was divided into three cells named A, B and C. Cell A was not used in this study, Cell B retained the model sand and shafts, and Cell C kept the excavated sand. The dimensions of Cell B were 200mm wide, 300mm deep and 200mm thick.

Figure 3 shows the special vacuum excavator, which consisted of an excavation pipe and an aspirator. The excavation pipe, whose dimensions were 22mm in inner diameter, 0.5mm in thickness and 265mm in length, had 45 lateral holes of 4mm diameter on its surface and a 4.5mm diameter polymer tube providing an air route within the excavation

pipe. This excavation pipe stood at the centre of Cell B. Negative pneumatic pressure was supplied at the bottom of the excavation pipe with the aspirator installed inside Cell C. The sand in the excavation pipe was sucked out due to the applied negative pressure from there to Cell C through the aspirator. As the level of the surface of the sand in the excavation pipe was lowered, sand particles at the surface of the sand in the shaft were progressively fed to the excavation pipe through the highest lateral holes. The authors verified under the gravitational acceleration field that this technique reproduced the excavation sequence which proceeded from the surface toward the bottom of the sand in the shaft.

The sand used in centrifuge model tests was air dried Toyoura sand which is a uniform fine sand. Properties of the sand were determined by means of method described in Japanese Society of Soil Mechanics and Foundation Engineering (1990), and the values are tabulated in Table 2. The sand was poured into Cell B through air from a hopper placed at 75cm high. When the thickness of the poured sand reaches 9cm, the model shaft was placed vertically at the centre of Cell B. The successive pouring was done up to 26cm thick, and both inside and outside of the shaft were filled with the poured sand.

After pouring, the surface of the sand was scraped in order to coincide with the circumferential plane corresponding to the radius from the axis of the centrifuge to the sand surface. The weight and the thickness of the sand were measured, and values of initial void ratio e_0 were calculated. Because the sand under centrifugal force field is subjected to self-weight compression, in-flight void ratios e were estimated with the following equation (Ueno et al. 1994).

$$e = 0.92e_0 + 0.041 \qquad (5)$$

After an imposed four cycles of accelerating to 100g and decelerating down to 1g, the sand and the shaft were accelerated to 100g. The sand in the shaft was then excavated with the special vacuum excavator, and the increments of circumferential strain of the shaft $\Delta\varepsilon_\theta$ were measured.

Table 2: Properties of Toyoura sand

Specific density	ρ_s	2.650	(g/cm^3)
Maximum dry density	ρ_{dmax}	1.660	(g/cm^3)
Minimum dry density	ρ_{dmin}	1.343	(g/cm^3)
Uniformity coefficient	U_c	1.40	
Internal friction angle	ϕ_d	40.5†	(°)

†CD test result: D_r=83.5%, σ'_c=196kPa

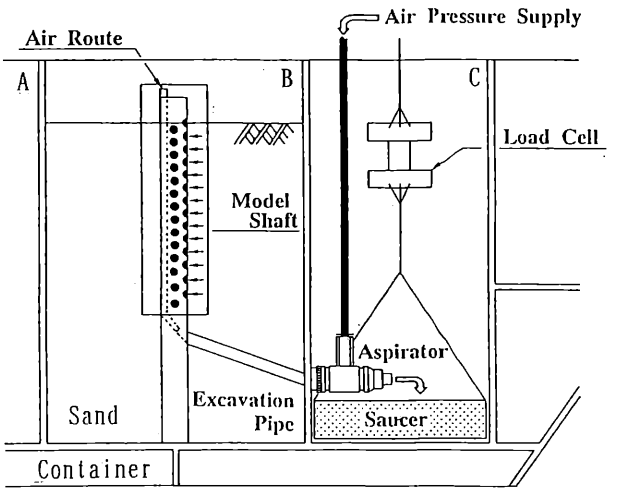

Fig. 3: Soil container and vacuum excavator

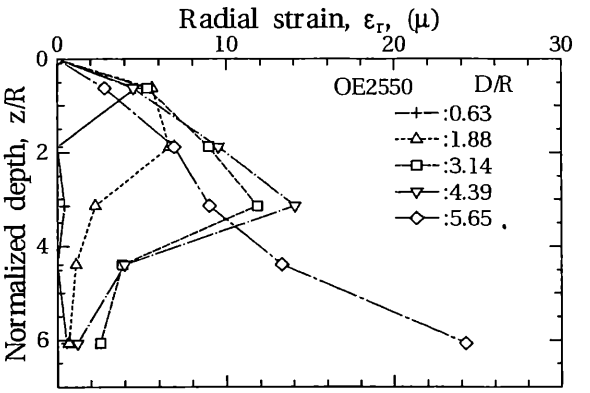

Fig. 4: Changes of the distribution of radial strain ε_r during an excavation process

4 RESULTS AND DISCUSSIONS

4.1 *Deformation of shafts*

Figure 4 shows changes in distributions of the radial strain ε_r induced in OE2550 model shaft during an excavation process under 100g (980m/s^2) of centrifuge acceleration. The point which shows the highest radial strain becomes deeper as the normalized excavation depth D/R becomes deeper. Because the inner wall of the shaft was supported by the internal sand, radial strains ε_r at the points deeper than excavated depth D were small.

4.2 *Effects of radius*

Figure 5 shows distributions of the radial earth pressure σ_r normalized by $\gamma_d R$ acting on three vertical cylindrical shafts with different radius R

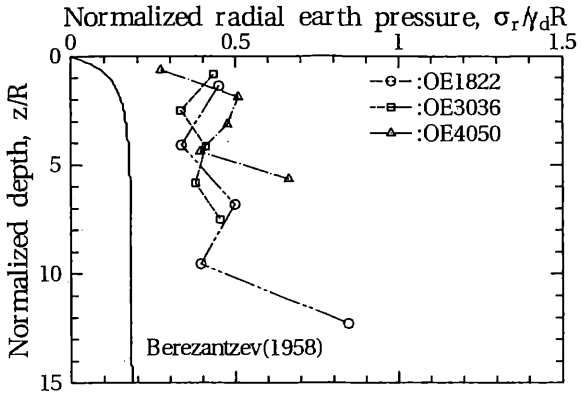

Fig. 5: Effects of radius

and identical apparent Young's modulus Et/R versus normalized depth z/R, where γ_d is the unit weight of the sand; R, the radius of the shafts; z, the depth. Reading out maximum values of radial strain produced at a particular observed depth, we obtained the distributions of the radial earth pressure.

Berezantzev (1958) derived the simplified expression for evaluating stresses acting on a vertical cylindrical surface. Eliminating the terms of surcharge and cohesion, we can introduce;

$$\sigma_{rB} = \gamma R \frac{\sqrt{K_a}}{\lambda - 1} \left\{ 1 - \left(\frac{R}{R + z\sqrt{K_a}} \right)^{\lambda - 1} \right\} \qquad (6)$$

where σ_{rB} is active earth pressure; R, the radius of the shaft; γ, the unit weight of the soil; K_a, Rankine's earth pressure coefficient and $K_a = \tan^2(45° - \phi/2)$; $\lambda = 2\tan\phi\tan(45° + \phi/2)$. The values predicted by Berezantzev (1958) are also presented in Fig. 5.

There being no noticeable difference between the values of $\sigma_r/\gamma_d R$ obtained from the shafts with different radii and identical stiffness implies that radial earth pressure σ_r tends to be in proportion to $\gamma_d R$. Plots are concentrated at from $\sigma_r/\gamma_d R$=0.3 to $\sigma_r/\gamma_d R$=0.5 except at the deepest point, and from 1.9 to 4.7 times greater than the value obtained from Berezantzev's prediction. It can be expected that the stiffness of the shafts is large enough to restrict radial deformations of the shafts, and that the soil surrounding the shafts is not fully yielded.

4.3 *Effects of stiffness*

Figure 6 shows the values of $\sigma_r/\gamma_d R$ obtained from five model shafts with different apparent Young's modulus Et/R and an identical radius R_p = 4.78m. The active earth pressures predicted by means of the Berezantzev and Rankine methods, and the at-rest pressure predicted by means of Jáky's method, computed with $\phi_d = 40.5°$, are also presented in this figure.

The values of $\sigma_r/\gamma R$ tend to become greater as apparent Young's modulus Et/R increases. This tendency is clearly observed over the shallower half. The values obtained from OE30AC model shaft are relatively small and close to the Berezantzev's value. On the other hand, the values from OE4050 model shaft are about two to five times the greater than the Berezantzev's value. You can see in this case that Berezantzev's prediction provides underestimation while Rankine's active earth pressure provides overestimation at deep sections. Because the deformations of surrounding soil were restricted by the shaft wall, the measured normalized radial earth pressure $\sigma_r/\gamma_d R$ becomes larger than the active earth pressure predicted by Berezantzev (1958). The results imply that the stiffness of the shafts dominates how much radial pressure acts on the shaft.

The plots of normalized radial earth pressure $\sigma_r/\gamma_d R$ observed at the shallowest and the deepest sections are rather high, except for the results obtained from OE30AC model shaft. Stress redistribution due to vertical arching effect may appear at these sections.

Figure 7 indicates how much the values of measured radial earth pressure σ_r are larger than Berezantzev's active earth pressure σ_{rB}. The ratio of measured radial earth pressure σ_r to Berezantzev's values σ_{rB} is denoted with α in Fig. 7. The values of α for envelope curves of σ_r, which is in proportion to Berezantzev's active earth pressure σ_{rB}, and which will be demonstrated in Fig. 8, were determined when the largest five plots measured at z/R = 0.63 and z/R = 5.56 are neglected. Applying least square method to the values of α of the envelope curves, we obtain;

$$\alpha = 1.15 \times 10^{-4} \frac{Et/R}{\sigma_a} + 1 \qquad (7)$$

where σ_a is a datum stress, which equals to 98kPa in SI system.

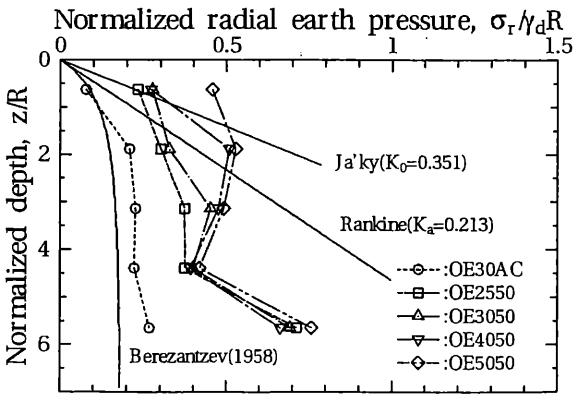

Fig. 6: Effects of stiffness

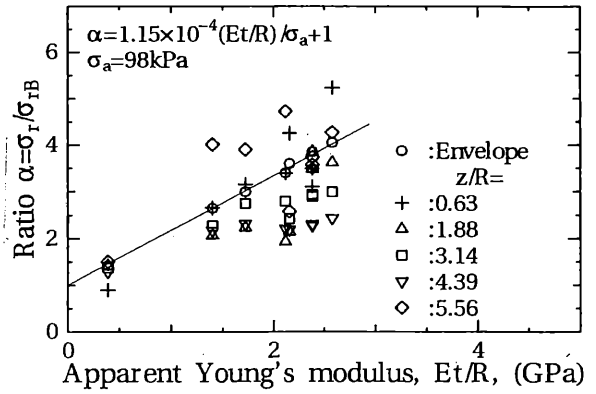

Fig. 7: Ratio α versus apparent Young's modulus

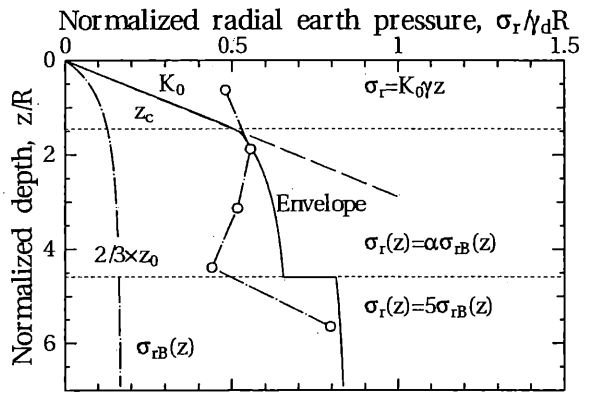

Fig. 8: Empirical prediction method

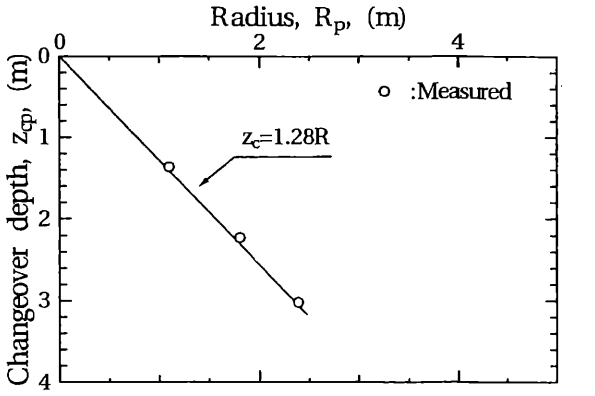

Fig. 9: Changeover depth z_c versus radius of shaft R

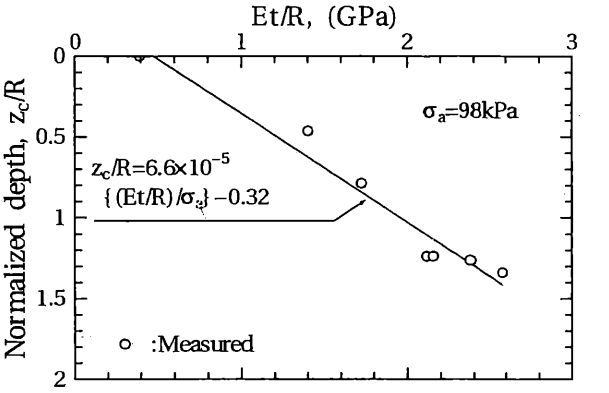

Fig. 10: Changeover depth z_c versus apparent Young's modulus Et/R

4.4 *An empirical prediction method*

An empirical prediction method for radial earth pressure σ_r was made in this study. The concept of this method is demonstrated in Fig. 8.

Firstly, it is assumed that the soil at the section shallower than a changeover depth is kept under K_0 condition because the radial earth pressure and the deformation of shafts are sufficiently small at shallow sections. The changeover depth, denoted with z_c in Fig. 8, was determined by means of either interpolation or extrapolation with envelope curves which were in proportion to the active earth pressure predicted by means of Berezantzev method σ_{rB}. Figure 9 shows the variation of the changeover depth z_c with the radius of shafts R. Plots indicate that the changeover depth z_c is in proportion to the radius of shafts R. Figure 10 also shows the relationship between the normalized changeover depth z_c/R and the apparent Young's modulus Et/R; the normalized changeover depth z_c/R increases with increasing apparent Young's modulus Et/R. Fortunately, the relationship is obedient and easily expressed with a linear function of Et/R; that is,

$$z_c/R = 6.6 \times 10^{-5} \frac{Et/R}{\sigma_a} - 0.32 \qquad (8)$$

The coefficient and the constant in Eq. 8 were determined by means of least squares.

Secondly, it was also assumed that the ratio of radial earth pressure σ_r to Berezantzev's active earth pressure σ_{rB}, denoted with α and expressed in Eq. 7, was kept constant along the depth down from the changeover depth z_c.

Thirdly, the stress redistribution due to vertical arching effect appears at the deepest one third of the embedded depth of the shaft z_0. Experimental results presented by Lade et al. (1981) and Fujii et al. (1994) and theoretical consideration suggested by Wong and Kaiser (1988a) and Wong and Kaiser (1988b) also indicated the rise of radial earth pressure at this deepest section. Regarding these results, the authors recommend that the ratio α at the deepest section should be increased and given a value at least 5.0.

Finally, we obtain an expression for the radial earth pressure σ_r.

$$\sigma_r(z) = \begin{cases} K_0\gamma_d z & (z \le z_c) \\ \alpha\sigma_{rB}(z) & (z_c < z \le \frac{2}{3}z_0) \\ 5\sigma_{rB}(z) & (\frac{2}{3}z_0 < z \le z_0) \end{cases} \qquad (9)$$

Distributions of radial earth pressure σ_r presented in

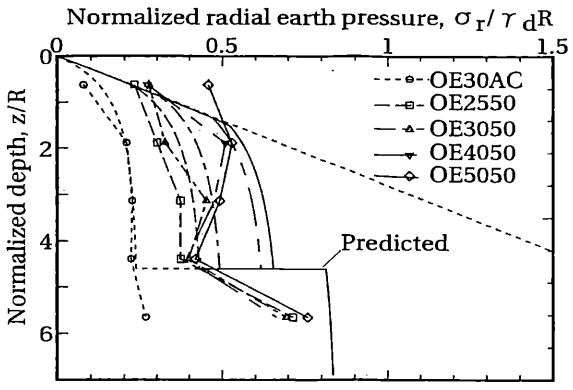

Fig. 11: Predicted and measured distributions of $\sigma_r/\gamma_d R$

Fig. 6 are again plotted in Fig. 11, together with predicted distributions. It can be concluded that the empirical prediction method presented in this paper provides a conservative prediction of radial earth pressure.

5 CONCLUSIONS

The effects of shaft stiffness on the radial earth pressures acting on flexible circular shafts were investigated by using a newly developed in-flight excavation technique for centrifuge model tests. The following conclusions were drawn from the test results.

1. Berezantzev's active earth pressure gave an underestimation, while Rankine's value was unduly conservative at deep sections.

2. No observable influence of the radius of shaft could be observed in normalized radial earth pressure $\sigma_r/\gamma R$. The earth pressure σ_r tends to be in proportion to both the unit weight γ of the soil and the radius of the shaft R.

3. Normalized radial earth pressure $\sigma_r/\gamma R$ increased as the apparent Young's modulus Et/R became larger. The stiffness of the shafts dominates the magnitude of the earth pressure. The ratio of the earth pressure σ_r to Berezantzev's active earth pressure σ_{rB} is expressed as

$$\alpha = 1.15 \times 10^{-4} \frac{Et/R}{\sigma_a} + 1$$

where σ_a is a datum stress and equals to 98kPa. The effects of stiffness should be considered in rational design methods.

4. An empirical prediction method regarding the effects of the stiffness of shafts was proposed in this study. This method provides rational conservative prediction of the earth pressure.

ACKNOWLEDGEMENT

The study presented here is a part of the outcome of an industrial joint research programme between Nishimatsu Construction Co., Ltd. and Utsunomiya University. The writers are grateful to Dr. Y. Imaizumi, Utsunomiya University, Prof. O. Kusakabe, Hiroshima University, Dr. T. Hagiwara, Gunma University, Mr. Y. Nomoto, Mr. K. Mito and Mr. S. Imamura, Nishimatsu Construction Co., Ltd. for their support and discussion.

REFERENCES

Berezantzev, V. (1958). Earth pressure on the cylindrical retaining walls. *Conference on Earth Pressure Problems, Brussels 2*, 21–24.

Fujii, T., T. Hagiwara, K. Ueno, and A. Taguchi (1994). Experiment and analysis of pressure on an axisymmetric shaft in sand. *Proc. of the Int. Conf. Centrifuge 94*, 791–796.

Japanese Society of Soil Mechanics and Foundation Engineering (1990). *Procedures and interpretations of soil testing.* Japanese Society of Soil Mechanics and Foundation Engineering. (in Japanese).

Lade, P. V., H. L. Jessberger, E. Makowski, and P. Jorden (1981). Modeling of deep shaft in centrifuge tests. *Proc. 10th International Conference on Soil Mechanics and Foundation Engineering 1*, 683–691.

Roark, R. J. and W. C. Young (1975). *Formulas for Stress and Strain* (2 ed.). McGraw-Hill Kogakusha Ltd.

Terzaghi, K. (1942). *Theoretical Soil Mechanics.* John Wiley and Sons Inc.

Ueno, K., T. Nakatomi, K. Mito, and O. Kusakabe (1994). Influence of initial conditions on bearing characteristics of sand. *Proc. of the Int. Conf. Centrifuge 94*, 541–546.

Wong, R. and P. K. Kaiser (1988a). Design and performance evaluation of vertical shafts: rational shaft design method and verification of design method. *Canadian Geotechnical Jour. 25*, 320–337.

Wong, R. and P. K. Kaiser (1988b). Design and performance evaluation of vertical shafts: reevaluation of model test results and evaluation of field measurements. *Canadian Geotechnical Jour. 25*, 338–352.